Robotica (2013) volume 31, pp. 183–191. © Cambridge University Press 2012
doi:10.1017/S0263574712000215

Kinematics/statics and workspace analysis of a 3-leg 5-DoF parallel manipulator with a UPU-type composite active constrained leg

Yi Lu†,*, Xuili Zhang‡, Chunping Sui§, Jianda Han§ and Bo Hu†

†*Robotics Research Centre, School of Mechanical Engineering, Yanshan University, Qinhuangdao, Hebei 066004, PR China*
‡*College of Qinhuangdao Building Material, Qinhuangdao, Hebei 066004, PR China*
§*State Key Laboratory of Robotics (Shenyan Institute of Automation, Chinese Academy of Sciences), Liaoning 110016, PR China*

(Accepted April 13, 2012. First published online: May 17, 2012)

SUMMARY
A novel 3-leg 5-DoF parallel manipulator (PM) with a UPU-type composite active constrained leg is proposed and its kinematics and statics are analyzed systematically. First, the formulae are derived for solving the inverse/forward displacements, inverse/forward velocities, and active/constraint forces. Second, the formulae are derived for solving inverse/forward accelerations. Third, a simulation mechanism of this PM is created and its workspace is constructed and analyzed. Finally, the analytic results are verified by its simulation mechanism.

KEYWORDS: Parallel manipulator; Kinematics; Active force; Constraint force; Workspace.

Nomenclature

DoF	Degree of freedom.
PM	Parallel manipulator.
m, B	The moving platform and the fixed base.
o, O	The central point of m and B.
a_i, A_i	The vertices of m and B ($i = 1, 2, 3$).
e_i	The line from a_i to o, $e_i = e$.
E_i	The line from A_i to O, $E_i = E$.
r_i	The active leg and its length.
l_i, L_i	The side of m and B.
P, S	The prismatic joint and the spherical joint.
R_j	The revolute joints ($j = 1, 2, 3, 4$).
U_m	The universal joint with R_1 and R_2.
U_B	The universal joint with R_3 and R_4.
$\{m\}$	Coordinate frame o-xyz fixed on m.
$\{B\}$	Coordinate frame O-XYZ fixed on B.
v_{ri}	The input velocity of active leg.
e, E	The distances from a_i to o and from A_i to O.
$\boldsymbol{F}$, $\boldsymbol{T}$	The concentrated force and torque applied on m at o.
$\boldsymbol{F}_{ai}$	The active forces applied on and along r_i.
$\boldsymbol{T}_a$	The active torque applied on R_1.
$\boldsymbol{T}_\lambda$	The active torque applied on R_4.
F_c, T_c	The constrained force and the constrained torque.
$\boldsymbol{T}_b$	The bending moment exerted on r_2.
$\boldsymbol{\delta}_i$, $\boldsymbol{c}$	The unit vectors of r_i and F_c.
$\mathbf{R}_m^B$	Rotational matrix from $\{m\}$ to $\{B\}$.
$\mathbf{J}$, $\mathbf{H}$	The Jacobian matrix and Hessian matrix.
x_l, x_m, x_n, y_l, y_m, y_n, z_l, z_m, z_n	Nine orientation parameters of m.
α, β, λ	3 Euler angles of m about (R_1, R_2, R_4).
X_o, Y_o, Z_o	The position components of o in $\{B\}$.
$\boldsymbol{V}$	The forward general velocity, $\boldsymbol{V} = [\boldsymbol{v}\boldsymbol{\omega}]^T$.
$\boldsymbol{A}$	The forward general acceleration, $\boldsymbol{A} = [\boldsymbol{a}\boldsymbol{\varepsilon}]^T$.
W	The reachable workspace.
$\parallel$, $\perp$	Parallel and perpendicular constraint.

* Corresponding author. E-mail: luyi@ysu.edu.cn

1. Introduction

Some parallel manipulators (PMs) have been utilized for many practical applications.[1,2] Among them, some 5-DoF PMs have attracted a lot of attentions for their merits, such as large workspace, larger capability of load bearing, and suitable for 3D free-form surface normal machining.[3–11] Generally, a conventional n-DoF PM ($n < 6$) includes a moving platform m, a fixed base B, n active legs, and 6-n couple structure constraints which are formed from two legs or more. Therefore, some conventional PMs may be highly sensitive to the manufacturing error due to 6-n couple structure constraints, and an unnecessary tiny self-motion of platform may be generated.[12,13] When rotating some joints connecting the active legs with B, the stability and the capability of load bearing of PMs may be increased and the force situations can be improved. Thus, some n-DoF PMs with the composite rotational/linear active legs have larger workspace, better flexibility, and fewer legs for avoiding interferences easily. In addition, the unnecessary tiny self-motion may be eliminated by the composite active constrained legs for increasing precision; more actuators can be installed onto the base for reducing vibration.[1,4] In this aspect, Fang and Tsai synthesized some 5-DoF PMs by screws theory.[3] Kong and Gosselin synthesized some 5-DoF PMs based on screw theory.[4] Huang *et al.* studied the dimension synthesis of 3-DoF TriVariant for a 5-DoF reconfigurable hybrid robot.[5] Adopting Lie group of displacements, Huang and Li synthesized some 5-DoF

PMs with three rotations plus two translations.[6] Gao *et al.* synthesized kinematic structures of some 5-DoF PMs using composite pairs and subchains.[7] Alizade and Bayram presented a revised method and formulation for designing some 5-DoF PMs with single and multiple platforms.[9] Lu *et al.* proposed a 5-DoF 4SPS+SPR parallel machine tool for 3D free-form surface normal machining.[10,11] In aspect of statics, Dasgupta solved the inverse dynamics by Newton–Euler formulation.[14] Tsai solved inverse dynamics of a Stewart–Gough PM by virtual work principle.[15] Gallardo analyzed dynamics of PMs by screw theory.[16] Dai *et al.*[17] analyzed statics of some over constrained PMs. Lu,[18] Gregorio,[19] and Huang[20] studied kinematics and statics of some 3-DoF PMs with UPU-type legs using different approaches. Using vector analytic approach or Lagrange equations, others studied the kinematics and dynamics of PMs.[21–23] It is confirmed by the experiments of a PM prototype with variable DoF and configuration in Yanshan University that using a constrained leg, the tiny self-motion of some PMs can be removed effectively. In this aspect, Zhang and Gosselin proposed *n*-DoF PMs with a central passive constrained leg.[8] Huang *et al.* studied two 3-DoF PMs, i.e., a Tricept with a central UP passive constrained leg and a TriVariant with a UP active constrained leg.[24] Güursel and Bijan analyzed a 3-SPS PM with a central passive constrained spherical joint.[25]

However, the central passive constrained leg also brings about some disadvantages. It increases the complexity of the structure and the possibility of interference among legs and the platform; it also reduces the effective workspace. In order to remove the tiny self-motion of *n*-DoF PMs, a novel 3-leg 5-DoF 2SPS+UPU PM with a UPU-type composite active constrained leg is proposed in this paper. Since *m* of this PM is only supported by three linear legs, the whole structure is simplified, the interference among the active legs and *m* can be avoided easily, and the workspace may be increased. In addition, two SPS-type legs in this PM only provide active forces and do not generate any structure constraints, and one UPU-type leg generates both the active forces/torques and the structure constraints in series. Since the structure constraint in series is not sensitive to the manufacturing error similar to one in series robot, the unnecessary tiny self-motion may be eliminated by the composite active constrained legs for increasing precision; more actuators can be installed onto the base for reducing vibration.[1,4]

In the light of merits of this unique asymmetric PM, this paper systematically studies its kinematics, statics, and workspace because this PM has some potential applications for parallel machine tools, sensors, surgical manipulators, tunnel borers, barbette of war ships, and satellite surveillance platforms.

2. Displacement Kinematics

2.1. Characteristics of 2SPS+UPU PM and its DoFs

A prototype of the 2SPS+UPU PM is shown in Fig. 1. It is composed of a moving platform *m*, a fixed base *B*, and two SPS (spherical joint-prismatic joint-spherical joint) active legs r_i ($i = 1, 3$) with the linear actuators, and one UPU

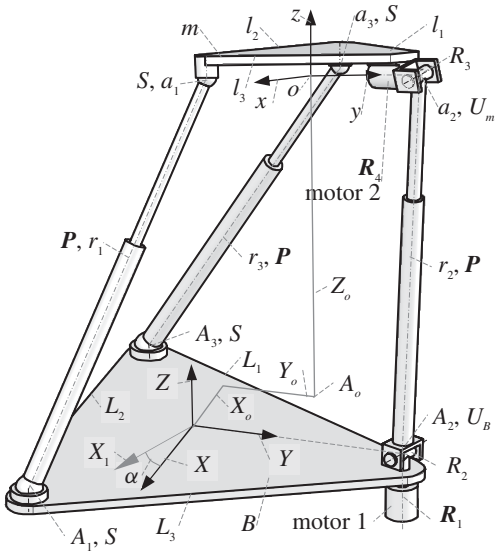

Fig. 1. A prototype of 2SPS+UPU PM.

(universal joint-prismatic joint-universal joint) composite active leg r_2 with a linear actuator and two rotational actuators (motor 1 and motor 2). Here, *m* is an equilateral ternary link $\Delta a_1a_2a_3$ with three sides $l_i = l$, three vertices a_i, and a central point *o*. *B* is an equilateral ternary link $\Delta A_1A_2A_3$ with three sides $L_i = L$, three vertices A_i, and a central point *O*. Let $\{m\}$ be a coordinate frame *o-xyz* fixed on *m* at *o*. Let $\{B\}$ be a coordinate frame *O-XYZ* fixed on *B* at *O*. Let $\perp$ be the perpendicular constraint and $\parallel$ be the parallel constraint. Each of SPS-type active legs r_i ($i = 1, 3$) connects *m* to *B* by a spherical joint *S* at a_i, an active leg r_i with a prismatic joint $\boldsymbol{P}$, and an *S* at A_i. The UPU-type composite active leg r_2 connects *m* to *B* by a universal joint U_m attached to *m* at a_2, an active leg r_2 with a $\boldsymbol{P}$, and a universal joint U_B attached to *B* at A_2. U_B is composed of two cross-revolute joints $\boldsymbol{R}_1$ and R_2. U_m is composed of two cross-revolute joints R_3 and $\boldsymbol{R}_4$. Here, active joints are marked by bold symbol. The geometric constrains ($R_1 \perp B$, $R_1 \perp R_2$, $R_2 \parallel R_3$, $R_3 \perp R_4$, $R_2 \perp r_2$, $R_3 \perp r_2$, and R_4 coinciding with *y*) are satisfied. In addition, $\boldsymbol{R}_1$ and $\boldsymbol{R}_4$ are connected with the motor 1 and the motor 2, respectively.

In the 2SPS+UPU PM, the number of links is $k = 8$ for one platform, three cylinders, three piston-rods, and one base; the number of joints is $g = 9$ for three prismatic joints, and two universal joints, and four spherical joints; the passive DoF is $M_0 = 2$ for two SPS-type active legs rotating about their won axes, and M_0 has no influence on the kinematic characteristics. Using a revised Kutzbach–Grübler equation,[1,2] the DoF of this PM is calculated as below

$$M = 6(k - g - 1) + \sum_{i=1}^{g} m_i - M_0 = 6 \times (8 - 9 - 1) + (3 \times 1 + 2 \times 2 + 4 \times 3) - 2 = 5. \quad (1)$$

As there are only three linear active legs, the 5-DoF 2SPS+UPU PM is obviously simple in structure and easy to avoid interference among active legs and *m*. Since the

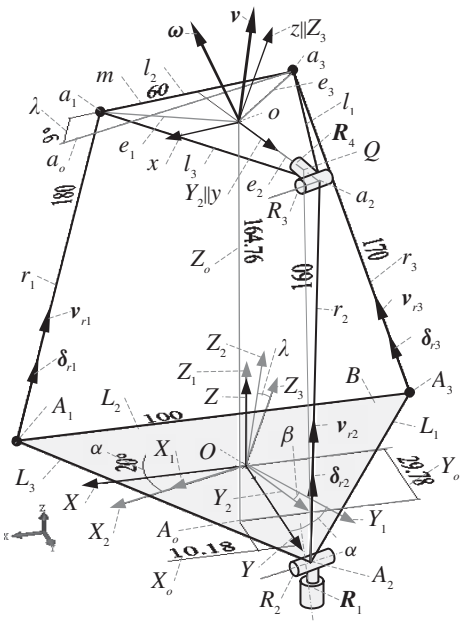

Fig. 2. A simulation mechanism with coordinate frames.

UPU-type constrained active leg r_2 provides prescribed 5-DoF serial motion and constrained force/torque to m, the tiny self-motion of m can be removed effectively.

In order to verify analytic results and solve workspace, a simulation mechanism of the 2SPS+UPU PM with relevant coordinate frames is constructed, see Fig. 2. The construction processes are explained in Appendix.

2.2. *Inverse displacement kinematics*

The coordinates $\boldsymbol{A}_i$ of A_i in $\{B\}$ and the coordinates ${\boldsymbol{a}_i}^m$ and $\boldsymbol{a}_i$ of a_i in $\{m\}$ and $\{B\}$ are expressed as follows:[1,2]

$$\boldsymbol{A}_i = \begin{bmatrix} X_{Ai} \\ Y_{Ai} \\ Z_{Ai} \end{bmatrix}, \quad \boldsymbol{a}_i^m = \begin{bmatrix} x_{ai} \\ y_{ai} \\ z_{ai} \end{bmatrix}, \quad \boldsymbol{a}_i = \begin{bmatrix} X_{ai} \\ Y_{ai} \\ Z_{ai} \end{bmatrix}, \quad \boldsymbol{o} = \begin{bmatrix} X_o \\ Y_o \\ Z_o \end{bmatrix},$$

$$\mathbf{R}_m^B = \begin{bmatrix} x_l & y_l & z_l \\ x_m & y_m & z_m \\ x_n & y_n & z_n \end{bmatrix}, \quad \boldsymbol{a}_i = \mathbf{R}_m^B \boldsymbol{a}_i^m + \boldsymbol{o}. \tag{2}$$

Here, $\boldsymbol{o}$ is a vector of point o on m in $\{B\}$, (X_o, Y_o, Z_o) are the components of $\boldsymbol{o}$; $\mathbf{R}_m^B$ is a rotation transformation matrix from $\{m\}$ to $\{B\}$; $(x_l, x_m, x_n, y_l, y_m, y_n, z_l, z_m, z_n)$ are the nine orientation parameters of m in $\{B\}$, they can be determined as shown in refs. [1, 2]. ${\boldsymbol{a}_i}^m$, $\boldsymbol{a}_i$, and $\boldsymbol{A}_i$ $(i = 1, 2, 3)$ are derived from Eq. (2) as:

$$\boldsymbol{a}_1^m = \frac{e}{2}\begin{bmatrix} b \\ -1 \\ 0 \end{bmatrix}, \quad \boldsymbol{a}_2^m = \begin{bmatrix} 0 \\ e \\ 0 \end{bmatrix}, \quad \boldsymbol{a}_3^m = \frac{e}{2}\begin{bmatrix} -b \\ -1 \\ 0 \end{bmatrix},$$

$$b = \sqrt{3}, \quad \boldsymbol{a}_1 = \frac{1}{2}\begin{bmatrix} bex_l - ey_l + 2X_o \\ bex_m - ey_m + 2Y_o \\ bex_n - ey_n + 2Z_o \end{bmatrix},$$

$$\boldsymbol{a}_3 = \frac{1}{2}\begin{bmatrix} -bex_l - ey_l + 2X_o \\ -bex_m - ey_m + 2Y_o \\ -bex_n - ey_n + 2Z_o \end{bmatrix}, \quad \boldsymbol{a}_2 = \begin{bmatrix} ey_l + X_o \\ ey_m + Y_o \\ ey_n + Z_o \end{bmatrix},$$

$$\boldsymbol{A}_1 = \frac{E}{2}\begin{bmatrix} b \\ -1 \\ 0 \end{bmatrix}, \quad \boldsymbol{A}_2 = \begin{bmatrix} 0 \\ E \\ 0 \end{bmatrix}, \quad \boldsymbol{A}_3 = \frac{E}{2}\begin{bmatrix} -b \\ -1 \\ 0 \end{bmatrix}. \tag{3}$$

Here, e is the distance from a_i to o, $e_i = e$; E is the distance from A_i to O, $E_i = E$.

Under the geometric constraints of the UPU constrained active leg r_2, $\mathbf{R}_m^B$ is formed by three Euler rotations of (ZX_1Y_2), namely, a rotation of α about Z, i.e., R_1, followed by a rotation of β about X_1, i.e., R_2, and a rotation of λ about Y_2, i.e., R_4. Here, X_1 is formed by X rotating about Z by α, Y_2 is formed by Y_1 rotating about X_1 by β, see Fig. 2. Let φ be one of (α, β, λ), set $c_\varphi = \cos\varphi$, $s_\varphi = \sin\varphi$, $t_\varphi = \tan\varphi$. Thus, $\mathbf{R}_m^B$ is derived as below

$$\mathbf{R}_m^B = \begin{bmatrix} c_\alpha c_\lambda - s_\alpha s_\beta s_\lambda & -s_\alpha c_\beta & c_\alpha s_\lambda + s_\alpha s_\beta c_\lambda \\ s_\alpha c_\lambda + c_\alpha s_\beta s_\lambda & c_\alpha c_\beta & s_\alpha s_\lambda - c_\alpha s_\beta c_\lambda \\ -c_\beta s_\lambda & s_\beta & c_\beta c_\lambda \end{bmatrix}. \tag{4a}$$

Comparing Eq. (2) with Eq. (4a) we get

$$x_l = c_\alpha c_\lambda - s_\alpha s_\beta s_\lambda, \quad x_m = s_\alpha c_\lambda + c_\alpha s_\beta s_\lambda,$$
$$x_n = -c_\beta c_\lambda, \quad y_l = -s_\alpha c_\beta, \quad y_m = c_\alpha c_\beta, \quad y_n = s_\beta. \tag{4b}$$

Let $\boldsymbol{R}_j$ $(j = 1, 2, 3, 4)$ be the unit vectors of joints R_j. Based on the geometric constraints of r_2, it is known that $\boldsymbol{R}_j$ $(j = 1, 2, 4)$ are the same as the unit vectors of (Z, X_1, y), respectively. Under the geometric constraints $(\boldsymbol{R}_2 \perp \boldsymbol{R}_1, \boldsymbol{R}_2 \perp \boldsymbol{r}_2, \boldsymbol{R}_2 \| \boldsymbol{R}_3, \boldsymbol{R}_3 \perp \boldsymbol{r}_2, \boldsymbol{R}_3 \perp \boldsymbol{R}_4)$, $(\boldsymbol{R}_1, \boldsymbol{R}_4, \boldsymbol{r}_2)$ must lie in the same plane. Thus, a constraint equation is derived from Eq. (4b) as follows:

$$(\boldsymbol{R}_1 \boldsymbol{R}_4 \boldsymbol{r}_2) = \begin{vmatrix} 0 & 0 & 1 \\ y_l & y_m & y_n \\ X_{a2} - X_{A2} & Y_{a2} - Y_{A2} & Z_{a2} - Z_{A2} \end{vmatrix} = 0,$$
$$X_o = (Y_o - E)y_l / y_m = (E - Y_o)t_a. \tag{4c}$$

Each of r_i $(i = 1, 2, 3)$, the unit vector $\boldsymbol{\delta}_i$ of r_i and the vector $\boldsymbol{e}_i$ of line e_i are solved as follows:[1,2]

$$\boldsymbol{r}_i = |\boldsymbol{a}_i - \boldsymbol{A}_i|, \quad \boldsymbol{\delta}_i = \boldsymbol{r}_i / r_i, \quad \boldsymbol{e}_i = \boldsymbol{a}_i - \boldsymbol{o}. \tag{5a}$$

From Eqs. (2), (3), and (5a), r_i $(i = 1, 2, 3)$ are derived as follows:

$$\begin{aligned} r_1^2 &= X_o^2 + Y_o^2 + Z_o^2 + E^2 + 2e^2 - bEX_o + EY_o \\ &\quad + be(x_l X_o + x_m Y_o + x_n Z_o) \\ &\quad + eE(by_l + bx_m - 3x_l - y_m)/2, \\ r_2^2 &= X_o^2 + Y_o^2 + Z_o^2 + E^2 - e^2 - 2E(ey_m + Y_o), \\ r_3^2 &= X_o^2 + Y_o^2 + Z_o^2 + E^2 + 2e^2 + bEX_o + EY_o \end{aligned}$$

$$- be(x_l X_o + x_m Y_o + x_n Z_o)$$
$$- eE(by_l + bx_m + 3x_l + y_m)/2. \quad (5b)$$

From Eqs. (4b), (4c), and (5b), r_i are expressed by (α, β, λ, Y_o, Z_o) as:

$$\begin{aligned}
r_1^2 &= (E - Y_o)^2 t_a^2 + Y_o^2 + Z_o^2 + E^2 + 2e^2 + EY_o \\
&\quad + b(E - Y_o)t_a(ec_\alpha c_\lambda - es_\alpha s_\beta s_\lambda - E) + beD \\
&\quad + \frac{eE}{2}[bs_\alpha(c_\lambda - c_\beta) + (bc_\alpha + 3s_\alpha)s_\beta s_\lambda - c_\alpha(3c_\lambda + c_\beta)], \\
r_2^2 &= Z_o^2 - e^2 - 2eEc_\alpha c_\beta + (E - Y_o)^2/c_\alpha^2, \\
r_3^2 &= (E - Y_o)^2 t_a^2 + Y_o^2 + Z_o^2 + E^2 + 2e^2 + EY_o \\
&\quad - b(E - Y_o)t_a(ec_\alpha c_\lambda - es_\alpha s_\beta s_\lambda - E) - beD \\
&\quad - \frac{eE}{2}[bs_\alpha(c_\lambda - c_\beta) + (bc_\alpha - 3s_\alpha)s_\beta s_\lambda + c_\alpha(3c_\lambda + c_\beta)], \\
D &= Y_o s_\alpha c_\lambda + Y_o c_\alpha s_\beta s_\lambda - Z_o c_\beta c_\lambda. \quad (5c)
\end{aligned}$$

From Eqs. (2), (3), (4b), and (5a)–(5c), $\boldsymbol{\delta}_i$ and $\boldsymbol{e}_i$ can be expressed by five independent pose parameters (α, β, λ, Y_o, Z_o) as follows:

$$\boldsymbol{\delta}_1 = \frac{1}{2r_1}\begin{bmatrix} bex_l + es_\alpha c_\beta + 2(E - Y_o)t_a - bE \\ bex_m - ec_\alpha c_\beta + 2Y_o + E \\ -bec_\beta c_\lambda - ec_\alpha c_\beta + 2Z_o \end{bmatrix},$$

$$\boldsymbol{\delta}_3 = \frac{1}{2r_3}\begin{bmatrix} -bex_l + es_\alpha c_\beta + 2(E - Y_o)t_a + bE \\ -bex_m - ec_\alpha c_\beta + 2Y_o + E \\ bec_\beta c_\lambda - ec_\alpha c_\beta + 2Z_o \end{bmatrix},$$

$$\boldsymbol{\delta}_2 = \frac{1}{r_2}\begin{bmatrix} -es_\alpha c_\beta + (E - Y_o)t_a \\ ec_\alpha c_\beta + Y_o - E \\ es_\beta + Z_o \end{bmatrix}, \quad \boldsymbol{e}_1 = \frac{e}{2}\begin{bmatrix} bx_l - s_\alpha c_\beta \\ bx_m - c_\alpha c_\beta \\ -bc_\beta c_\lambda - s_\beta \end{bmatrix},$$

$$\boldsymbol{e}_2 = e\begin{bmatrix} -s_\alpha c_\beta \\ c_\alpha c_\beta \\ s_\beta \end{bmatrix}, \quad \boldsymbol{e}_3 = \frac{e}{2}\begin{bmatrix} -bx_l + s_\alpha c_\beta \\ -bx_m - c_\alpha c_\beta \\ bc_\beta c_\lambda - s_\beta \end{bmatrix},$$

$$x_l = c_\alpha c_\lambda - s_\alpha s_\beta s_\lambda, \quad x_m = s_\alpha c_\lambda + c_\alpha s_\beta s_\lambda. \quad (6)$$

When given (α, β, λ, Y_o, Z_o), r_i, $\boldsymbol{\delta}_i$, and $\boldsymbol{e}_i$ ($i = 1, 2, 3$) can be solved from Eqs. (5c) and (6). The results have been verified by its simulation mechanism.

3. Inverse/Forward Velocity and Jacobian Matrix

Let $\boldsymbol{V}$ and $\boldsymbol{v}_i$ be the velocities of platform m at o and a_i, respectively. They are expressed as follows:[1,2]

$$\boldsymbol{V} = \begin{bmatrix} \boldsymbol{v} \\ \boldsymbol{\omega} \end{bmatrix}, \quad \boldsymbol{v} = \begin{bmatrix} v_x \\ v_y \\ v_z \end{bmatrix}, \quad \boldsymbol{\omega} = \begin{bmatrix} \omega_x \\ \omega_y \\ \omega_z \end{bmatrix}, \quad \boldsymbol{v}_i = \boldsymbol{v} + \boldsymbol{\omega} \times \boldsymbol{e}_i. \quad (7)$$

Here, $\boldsymbol{v}$ and $\boldsymbol{\omega}$ are linear and angular velocities of m at o.

The velocities along active legs r_i ($i = 1, 2, 3$) are derived from Eq. (7) as follows:

$$\begin{aligned}
v_{ri} &= \boldsymbol{v}_i \cdot \boldsymbol{\delta}_i = (\boldsymbol{v} + \boldsymbol{\omega} \times \boldsymbol{e}_i) \cdot \boldsymbol{\delta}_i = \boldsymbol{\delta}_i \cdot \boldsymbol{v} + (\boldsymbol{e}_i \times \boldsymbol{\delta}_i) \cdot \boldsymbol{\omega} \\
\Rightarrow \begin{bmatrix} v_{r1} \\ v_{r2} \\ v_{r3} \end{bmatrix} &= \begin{bmatrix} \boldsymbol{\delta}_1^T & (\boldsymbol{e}_1 \times \boldsymbol{\delta}_1)^T \\ \boldsymbol{\delta}_2^T & (\boldsymbol{e}_2 \times \boldsymbol{\delta}_2)^T \\ \boldsymbol{\delta}_3^T & (\boldsymbol{e}_3 \times \boldsymbol{\delta}_3)^T \end{bmatrix}_{3\times 6} \boldsymbol{V}. \quad (8)
\end{aligned}$$

Let α be a rotational angle of m about R_1, i.e, Z. From Eqs. (2) and (4c), $\boldsymbol{R}_j$ ($j = 1, 2, 3, 4$) and $\boldsymbol{o}$ can be expressed as follows:

$$\boldsymbol{R}_1 = \begin{bmatrix} 0 \\ 0 \\ 1 \end{bmatrix}, \quad \boldsymbol{R}_2 = \boldsymbol{R}_3 = \begin{bmatrix} c_\alpha \\ s_\alpha \\ 0 \end{bmatrix},$$
$$\boldsymbol{R}_4 = \begin{bmatrix} -s_\alpha c_\beta \\ c_\alpha c_\beta \\ s_\beta \end{bmatrix}, \quad \boldsymbol{o} = \begin{bmatrix} (E - Y_o)t_a \\ Y_o \\ Z_o \end{bmatrix}. \quad (9)$$

Let $\dot{\alpha}$, $\dot{\beta}$, $\dot{\lambda}$ be three angular velocities of m about R_1, R_2, and R_4, respectively. Based on the geometric constraints of r_2, the angular velocity $\boldsymbol{\omega}$ of m is determined as

$$\boldsymbol{\omega} = \boldsymbol{R}_1\dot{\alpha} + \boldsymbol{R}_2\dot{\beta} + \boldsymbol{R}_4\dot{\lambda}. \quad (10a)$$

Dot-multiplying Eq. (10a) with $(\boldsymbol{R}_2 \times \boldsymbol{R}_3)$ at both sides yields

$$\begin{aligned}
\dot{\alpha} &= \frac{(\boldsymbol{R}_2 \times \boldsymbol{R}_4) \cdot \boldsymbol{\omega}}{(\boldsymbol{R}_2 \times \boldsymbol{R}_4) \cdot \boldsymbol{R}_1} = \frac{1}{c_\beta}[s_\alpha s_\beta \quad -c_\alpha s_\beta \quad c_\beta]^T \cdot \boldsymbol{\omega} \\
&= \begin{bmatrix} s_\alpha t_\beta & -c_\alpha t_\beta & 1 \end{bmatrix}\boldsymbol{\omega}. \quad (10b)
\end{aligned}$$

Similarly, the angular velocities $\dot{\beta}$ and $\dot{\lambda}$ of m about R_2 and R_4 are derived as follows:

$$\begin{aligned}
\dot{\beta} &= \frac{(\boldsymbol{R}_1 \times \boldsymbol{R}_4) \cdot \boldsymbol{\omega}}{(\boldsymbol{R}_1 \times \boldsymbol{R}_4) \cdot \boldsymbol{R}_2} = [c_\alpha \quad s_\alpha \quad 0]\,\boldsymbol{\omega}, \\
\dot{\lambda} &= \frac{(\boldsymbol{R}_1 \times \boldsymbol{R}_2) \cdot \boldsymbol{\omega}}{(\boldsymbol{R}_1 \times \boldsymbol{R}_2) \cdot \boldsymbol{R}_4} = \begin{bmatrix} -\frac{s_\alpha}{c_\beta} & \frac{c_\alpha}{c_\beta} & 0 \end{bmatrix}\boldsymbol{\omega}. \quad (10c)
\end{aligned}$$

Thus, $\dot{\alpha}$, $\dot{\beta}$, $\dot{\lambda}$ are expressed as follows:

$$\begin{bmatrix} \dot{\alpha} \\ \dot{\beta} \\ \dot{\lambda} \end{bmatrix} = \begin{bmatrix} s_\alpha t_\beta & -c_\alpha t_\beta & 1 \\ c_\alpha & s_\alpha & 0 \\ -s_\alpha/c_\beta & c_\alpha/c_\beta & 0 \end{bmatrix}\omega,$$

$$[\dot{\alpha} \quad \dot{\beta} \quad \dot{\lambda}] = \boldsymbol{\omega}^T \begin{bmatrix} s_\alpha t_\beta & -c_\alpha t_\beta & 1 \\ c_\alpha & s_\alpha & 0 \\ -s_\alpha/c_\beta & c_\alpha/c_\beta & 0 \end{bmatrix}^T,$$

$$\dot{\alpha} = [\boldsymbol{0}_{1\times 3} \quad \boldsymbol{q}_\alpha^T]\boldsymbol{V}, \quad \boldsymbol{q}_\alpha^T = [s_\alpha t_\beta \quad -c_\alpha t_\beta \quad 1],$$

$$\dot{\lambda} = [\boldsymbol{0}_{1\times 3} \quad \boldsymbol{q}_\lambda^T]\boldsymbol{V}, \quad \boldsymbol{q}_\lambda^T = \frac{1}{c_\beta}[-s_\alpha \quad c_\alpha \quad 0]. \quad (10d)$$

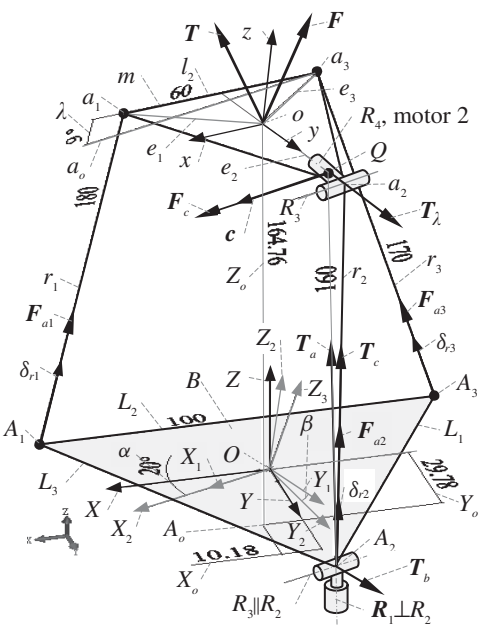

Fig. 3. Force situation of 2SPS+UPU PM.

The force situation of the 2SPS+RPU PM is shown in Fig. 3. Let $\boldsymbol{F}_c$ be a constrained force, $\boldsymbol{c}$ be the unit vector of $\boldsymbol{F}_c$, and $\boldsymbol{d}$ be the arm vector from point o to $\boldsymbol{F}_c$.

Since $\boldsymbol{F}_c$ do not do any work during the movement of m, there must be

$$F_c\boldsymbol{c}\cdot\boldsymbol{v}+(\boldsymbol{d}\times F_c\boldsymbol{c})\cdot\boldsymbol{\omega}=0\Rightarrow[\boldsymbol{c}^T\ (\boldsymbol{c}\times\boldsymbol{d})^T]\,\boldsymbol{V}=0. \tag{11a}$$

Let $\boldsymbol{v}_{r2}$ be a translation velocity along r_2, there must be $\boldsymbol{F}_c \cdot \boldsymbol{v}_{r2}=0$, i.e., $\boldsymbol{F}_c\perp r_2$. Let $\boldsymbol{\rho}_j\times\boldsymbol{F}_c$ be a torque of $\boldsymbol{F}_c$ about R_j ($j=1,2,3,4$), there must be $\boldsymbol{R}_j\cdot(\boldsymbol{\rho}_j\times\boldsymbol{F}_c)=0$. In this case, $\boldsymbol{F}_c$ must intersect or be parallel with every $\boldsymbol{R}_j$, respectively. In addition, based on the geometric constrains of ($R_2\perp R_1$, $R_2\perp r_2$, $R_2\|R_3$, $R_3\perp r_2$, $R_3\perp R_4$, and R_4 coinciding with y), (R_1, r_2, R_4) must lie in a plane Δoa_2A_2.

Based on these geometric constrains, $\boldsymbol{F}_c$ is determined to exert at a crossing point Q of R_1 and R_4, see Fig. 3. The unit vector $\boldsymbol{c}$ of $\boldsymbol{F}_c$ is determined as

$$\boldsymbol{c}=\boldsymbol{R}_2=\boldsymbol{R}_3=[c_\alpha\quad s_\alpha\quad 0]^T. \tag{11b}$$

A line equation of R_4, i.e., y in $\{B\}$ are derived as

$$(x-X_o)/y_l=(y-Y_o)/y_m=(z-Z_o)/y_n. \tag{11c}$$

Substituting a line equation $x=0$ and $y=E$ of R_1 into Eq. (11c), the coordinate of $\boldsymbol{Q}$ in $\{B\}$ is determined from Eq. (4b) as

$$\boldsymbol{Q}=\left[0\quad E\quad Z_o+(E-Y_o)\tfrac{t_\beta}{c_\beta}\right]^T. \tag{11d}$$

From Eqs. (3), (5c), and (11d), $\boldsymbol{Q}-\boldsymbol{a}_2$ and $\boldsymbol{d}$ are derived as follows:

$$\boldsymbol{Q}-\boldsymbol{a}_2=\left(\frac{E-Y_o}{c_\alpha}-ec_\beta\right)\begin{bmatrix}-s_\alpha\\ c_\alpha\\ t_\beta\end{bmatrix},$$

$$\boldsymbol{d}=\boldsymbol{Q}-\boldsymbol{o}=\frac{(E-Y_o)}{c_\alpha}\begin{bmatrix}-s_\alpha\\ c_\alpha\\ t_\beta\end{bmatrix}. \tag{11e}$$

Combining Eq. (8b) with Eqs. (10d) and (11a), the inverse/forward velocities and a Jacobian matrix **J** are derived as follows:

$$\begin{bmatrix}v_{r1}\\ v_{r2}\\ v_{r3}\\ \dot\alpha\\ \dot\lambda\\ 0\end{bmatrix}=J\boldsymbol{V},\quad \boldsymbol{V}=J^{-1}\begin{bmatrix}v_{r1}\\ v_{r2}\\ v_{r3}\\ \dot\alpha\\ \dot\lambda\\ 0\end{bmatrix},$$

$$J=\begin{bmatrix}\boldsymbol{\delta}_1^T & (\boldsymbol{e}_1\times\boldsymbol{\delta}_1)^T\\ \boldsymbol{\delta}_2^T & (\boldsymbol{e}_2\times\boldsymbol{\delta}_2)^T\\ \boldsymbol{\delta}_3^T & (\boldsymbol{e}_3\times\boldsymbol{\delta}_3)^T\\ \boldsymbol{0}_{1\times3} & \boldsymbol{q}_\alpha^T\\ \boldsymbol{0}_{1\times3} & \boldsymbol{q}_\lambda^T\\ \boldsymbol{c}^T & (\boldsymbol{d}\times\boldsymbol{c})^T\end{bmatrix}_{6\times6}. \tag{12a}$$

4. Active/Constrained Forces and Torque

In 2SPS+UPU PM, the workloads can be simplified as a wrench ($\boldsymbol{F}$,$\boldsymbol{T}$) applied onto m at o. Here, $\boldsymbol{F}$ is a concentrated force, $\boldsymbol{T}$ is a concentrated torque. ($\boldsymbol{F}$, $\boldsymbol{T}$) are balanced by three active forces $\boldsymbol{F}_{ai}$ ($i=1,2,3$) applied on and along active leg r_i, an active torque $\boldsymbol{T}_a$ applied on constrained active leg r_2 and about Z, an active torque $\boldsymbol{T}_\lambda$ applied on r_2 and about y, a constraint force $\boldsymbol{F}_c$ exerted on r_2 at point Q, see Fig. 3.

Based on principle of virtual work, the active/constraint forces and torques are derived from Eq. (12a) as follows:

$$\begin{bmatrix}F_{a1}\\ F_{a2}\\ F_{a3}\\ T_a\\ T_\lambda\\ F_c\end{bmatrix}^T\begin{bmatrix}v_{r1}\\ v_{r2}\\ v_{r3}\\ \dot\alpha\\ \dot\lambda\\ 0\end{bmatrix}+\begin{bmatrix}\boldsymbol{F}\\ \boldsymbol{T}\end{bmatrix}^T\boldsymbol{V}=0,\quad \begin{bmatrix}F_{a1}\\ F_{a2}\\ F_{a3}\\ T_a\\ T_\lambda\\ F_c\end{bmatrix}^T J+\begin{bmatrix}\boldsymbol{F}\\ \boldsymbol{T}\end{bmatrix}^T=0,$$

$$[F_{a1}\quad F_{a2}\quad F_{a3}\quad T_a\quad T_\lambda\quad F_c]^T=-(J^T)^{-1}\begin{bmatrix}\boldsymbol{F}\\ \boldsymbol{T}\end{bmatrix}. \tag{12b}$$

When both the constraint force $\boldsymbol{F}_c$ and the active torque $\boldsymbol{T}_\alpha$ are applied on r_2, a constrained torque $\boldsymbol{T}_c$ exerted on and along r_2 and a bending moment $\boldsymbol{T}_b$ are solved as follows:

$$T_c = -[(\boldsymbol{q} - \boldsymbol{a}_2) \times F_c\boldsymbol{c} + T_\alpha \boldsymbol{R}_1] \cdot \boldsymbol{\delta}_2, \quad T_b = F_c r_2. \quad (12c)$$

5. Inverse/Forward Acceleration

Suppose, there is a vector $\boldsymbol{\eta}$ and its skew-symmetric matrix $\hat{\boldsymbol{\eta}}$. Then it must satisfy[10]

$$\boldsymbol{\eta} = \begin{bmatrix} \eta_x \\ \eta_y \\ \eta_z \end{bmatrix}, \quad \hat{\boldsymbol{\eta}} = \begin{bmatrix} 0 & -\eta_z & \eta_y \\ \eta_z & 0 & -\eta_x \\ -\eta_y & \eta_x & 0 \end{bmatrix}, \quad \begin{matrix} \boldsymbol{\eta} \times = \hat{\boldsymbol{\eta}} \\ \hat{\boldsymbol{\eta}}^T = -\hat{\boldsymbol{\eta}} \\ \hat{\boldsymbol{\eta}}^2 = \hat{\boldsymbol{\eta}}\hat{\boldsymbol{\eta}} \end{matrix} \quad (13)$$

Here, $\boldsymbol{\eta}$ may be one of vectors $(\boldsymbol{e}_i, \boldsymbol{\delta}_i, \boldsymbol{c}, \boldsymbol{d})$, $i = 1, 2, 3$.

Let $\boldsymbol{A}$ be a general forward acceleration of m, $\boldsymbol{a}$ and $\boldsymbol{\varepsilon}$ be the linear and angular accelerations of m at o. They can be expressed as follows:

$$\boldsymbol{A} = \begin{bmatrix} \boldsymbol{a} \\ \boldsymbol{\varepsilon} \end{bmatrix}, \quad \boldsymbol{a} = \begin{bmatrix} a_x \\ a_y \\ a_z \end{bmatrix}, \quad \boldsymbol{\varepsilon} = \begin{bmatrix} \varepsilon_x \\ \varepsilon_y \\ \varepsilon_z \end{bmatrix}. \quad (14a)$$

The scalar velocities v_{ri} and accelerations a_{ri} of r_i along r_i $(i = 1, 2, 3)$ have been derived in ref. [10] as follows:

$$\begin{aligned} v_{ri} &= \boldsymbol{J}_{ri}\boldsymbol{V}, \quad a_{ri} = \boldsymbol{J}_{ri}\boldsymbol{A} + \boldsymbol{V}^T h_i \boldsymbol{V}, \\ \boldsymbol{J}_{ri} &= [\boldsymbol{\delta}_i^T \quad (\boldsymbol{e}_i \times \boldsymbol{\delta}_i)^T]_{1\times 6}, \quad i = 1, 2, 3, \\ \mathbf{h}_i &= \frac{1}{r_i}\begin{bmatrix} -\hat{\boldsymbol{\delta}}_i^2 & \hat{\boldsymbol{\delta}}_i^2\hat{\mathbf{e}}_i \\ -\hat{\mathbf{e}}_i\hat{\boldsymbol{\delta}}_i^2 & r_i\hat{\mathbf{e}}_i\hat{\boldsymbol{\delta}}_i + \hat{\mathbf{e}}_i\hat{\boldsymbol{\delta}}_i^2\hat{\mathbf{e}}_i \end{bmatrix}_{6\times 6}. \end{aligned} \quad (14b)$$

Here, $\mathbf{h}_i$ is the ith 6×6 sub-Hessian matrix.

Differentiating the fourth row of Eq. (12a) with respect to time, an angular acceleration $\ddot{\alpha}$ about Z is derived from Eq. (10d) as follows:

$$\begin{aligned} \ddot{\alpha} &= \begin{bmatrix} s_\alpha t_\beta \\ -c_\alpha t_\beta \\ 1 \end{bmatrix} \boldsymbol{\varepsilon} + [\dot{\alpha} \quad \dot{\beta} \quad \dot{\lambda}] \begin{bmatrix} c_\alpha t_\beta & s_\alpha t_\beta & 0 \\ s_\alpha/c_\beta^2 & -c_\alpha/c_\beta^2 & 0 \\ 0 & 0 & 0 \end{bmatrix} \boldsymbol{\omega} \\ &= \boldsymbol{q}_\alpha \cdot \boldsymbol{\varepsilon} + \boldsymbol{\omega}^T \mathbf{J}_\alpha \boldsymbol{\omega} = [\mathbf{0}_{1\times 3} \quad \boldsymbol{q}_\alpha]\boldsymbol{A} + \boldsymbol{V}^T \mathbf{h}_4 \boldsymbol{V}, \end{aligned} \quad (15a)$$

here

$$\mathbf{h}_4 = \begin{bmatrix} \mathbf{0}_{3\times 3} & \mathbf{0}_{3\times 3} \\ \mathbf{0}_{3\times 3} & \mathbf{J}_\alpha \end{bmatrix},$$

$$\mathbf{J}_\alpha = \begin{bmatrix} s_\alpha t_\beta & -c_\alpha t_\beta & 1 \\ c_\alpha & s_\alpha & 0 \\ -\dfrac{s_\alpha}{c_\beta} & \dfrac{c_\alpha}{c_\beta} & 0 \end{bmatrix}^T \begin{bmatrix} c_\alpha t_\beta & s_\alpha t_\beta & 0 \\ \dfrac{s_\alpha}{c_\beta^2} & -\dfrac{c_\alpha}{c_\beta^2} & 0 \\ 0 & 0 & 0 \end{bmatrix}. \quad (15b)$$

Differentiating the fifth row in Eq. (12a) with respect to time, from Eq. (10d), we get

$$\begin{aligned} \ddot{\lambda} &= \frac{1}{c_\beta}\begin{bmatrix} -s_\alpha \\ c_\alpha \\ 0 \end{bmatrix} \varepsilon + \frac{[\dot{\alpha} \quad \dot{\beta} \quad \dot{\lambda}]}{c_\beta} \begin{bmatrix} -c_\alpha & -s_\alpha t_\beta & 0 \\ -s_\alpha t_\beta & c_\alpha t_\beta & 0 \\ 0 & 0 & 0 \end{bmatrix} \boldsymbol{\omega} \\ &= \boldsymbol{q}_\lambda \cdot \boldsymbol{\varepsilon} + \boldsymbol{\omega}^T \mathbf{J}_\lambda \boldsymbol{\omega} = [\mathbf{0}_{1\times 3} \quad \boldsymbol{q}_\lambda]\boldsymbol{A} + \boldsymbol{V}^T \mathbf{h}_5 \boldsymbol{V}, \end{aligned} \quad (15c)$$

here

$$\mathbf{h}_5 = \begin{bmatrix} \mathbf{0}_{3\times 3} & \mathbf{0}_{3\times 3} \\ \mathbf{0}_{3\times 3} & \mathbf{J}_\lambda \end{bmatrix}, \quad \mathbf{J}_\lambda = \frac{1}{c_\beta}\begin{bmatrix} s_\alpha t_\beta & -c_\alpha t_\beta & 1 \\ c_\alpha & s_\alpha & 0 \\ -\dfrac{s_\alpha}{c_\beta} & \dfrac{c_\alpha}{c_\beta} & 0 \end{bmatrix}^T \times \begin{bmatrix} -c_\alpha & -s_\alpha & 0 \\ -s_\alpha t_\beta & c_\alpha t_\beta & 0 \\ 0 & 0 & 0 \end{bmatrix}.$$

Differentiating the sixth row in Eq. (12a) with respect to time we get

$$\mathbf{0}_{1\times 6} = [\boldsymbol{c}^T \quad (\boldsymbol{d} \times \boldsymbol{c})^T]\boldsymbol{A} + [\dot{\boldsymbol{c}}^T \quad (\boldsymbol{d} \times \dot{\boldsymbol{c}})^T + (\dot{\boldsymbol{d}} \times \boldsymbol{c})^T]\boldsymbol{V}. \quad (16a)$$

Differentiating the first equation in Eq. (11b) with respect to time, from Eq. (10d), we get

$$\begin{aligned} \dot{\boldsymbol{c}} &= [-s_\alpha \quad c_\alpha \quad 0]^T \dot{\alpha} \\ &= [-s_\alpha \quad c_\alpha \quad 0]^T [s_\alpha t_\beta \quad -c_\alpha t_\beta \quad 1]\boldsymbol{\omega} = J_c \boldsymbol{\omega}, \\ J_c &= \begin{bmatrix} -s_\alpha^2 t_\beta & s_\alpha c_\alpha t_\beta & -s_\alpha \\ s_\alpha c_\alpha t_\beta & -c_\alpha^2 t_\beta & c_\alpha \\ 0 & 0 & 0 \end{bmatrix}. \end{aligned} \quad (16b)$$

From Eq. (10d), we get

$$\begin{bmatrix} \dot{\alpha} \\ \dot{\beta} \\ \dot{Y}_o \end{bmatrix} = \begin{bmatrix} 0 & 0 & 0 & s_\alpha t_\beta & -c_\alpha t_\beta & 1 \\ 0 & 0 & 0 & c_\alpha & s_\alpha & 0 \\ 0 & 1 & 0 & 0 & 0 & 0 \end{bmatrix} \boldsymbol{V}. \quad (16c)$$

Differentiating the second equation in Eq. (11e), from Eq. (16c), we get

$$\dot{\boldsymbol{d}} = \frac{1}{c_\alpha}\begin{bmatrix} -\dfrac{E - Y_o}{c_\alpha} & 0 & s_\alpha \\ 0 & 0 & -1 \\ (E - Y_o)t_\alpha t_\beta & \dfrac{E - Y_o}{c_\beta^2} & -t_\beta \end{bmatrix} \begin{bmatrix} \dot{\alpha} \\ \dot{\beta} \\ \dot{Y}_o \end{bmatrix} = \mathbf{J}_d \boldsymbol{V}, \quad (16d)$$

here

$$J_d = \frac{E - Y_o}{c_\alpha}\begin{bmatrix} 0 & \dfrac{s_\alpha}{E-Y_o} & 0 & -t_\alpha t_\beta & t_\beta & -\dfrac{1}{c_\alpha} \\ 0 & -\dfrac{1}{E-Y_o} & 0 & 0 & 0 & 0 \\ 0 & -\dfrac{t_\beta}{E-Y_o} & 0 & \dfrac{s_\alpha^2}{c_\alpha}t_\beta^2 + \dfrac{c_\alpha}{c_\beta^2} & s_\alpha & t_\alpha t_\beta \end{bmatrix}.$$

From Eqs. (13) and (16b), the second expression in Eq. (16a) is derived as follows:

$$\begin{aligned}(\dot{\boldsymbol{d}} \times \boldsymbol{c})^T + (\boldsymbol{d} \times \dot{\boldsymbol{c}})^T &= -(\hat{\mathbf{c}}\dot{\boldsymbol{d}})^T + (\hat{\mathbf{d}}\dot{\boldsymbol{c}})^T \\ &= -(\hat{\mathbf{c}}\mathbf{J}_d\boldsymbol{V})^T + (\hat{\mathbf{d}}\mathbf{J}_c\boldsymbol{\omega})^T = -\boldsymbol{V}^T(\hat{\mathbf{c}}\mathbf{J}_d)^T + \boldsymbol{\omega}^T(\hat{\mathbf{d}}\mathbf{J}_c)^T.\end{aligned} \tag{16e}$$

From Eqs. (16b)–(16e), we get

$$\begin{aligned}&\begin{bmatrix}\dot{\boldsymbol{c}}^T & \mathbf{0}_{1\times3}\end{bmatrix} = \begin{bmatrix}\boldsymbol{\omega}^T\mathbf{J}_c^T & \mathbf{0}_{1\times3}\end{bmatrix} = \boldsymbol{V}^T\begin{bmatrix}\mathbf{0}_{3\times3} & \mathbf{0}_{3\times3} \\ \mathbf{J}_c^T & \mathbf{0}_{3\times3}\end{bmatrix}, \\ &\begin{bmatrix}\mathbf{0}_{1\times3} & (\boldsymbol{d}\times\dot{\boldsymbol{c}})^T + (\dot{\boldsymbol{d}}\times\boldsymbol{c})^T\end{bmatrix} = -\boldsymbol{V}^T\begin{bmatrix}\mathbf{0}_{6\times3} & (\hat{\mathbf{c}}\mathbf{J}_d)^T\end{bmatrix} \\ &\quad + \boldsymbol{V}^T\begin{bmatrix}\mathbf{0}_{3\times3} & \mathbf{0}_{3\times3} \\ \mathbf{0}_{3\times3} & (\hat{\mathbf{d}}\mathbf{J}_c)^T\end{bmatrix}.\end{aligned} \tag{16f}$$

From Eq. (16f), we get

$$\begin{aligned}&[\dot{\boldsymbol{c}}^T \quad (\boldsymbol{d}\times\dot{\boldsymbol{c}})^T + (\dot{\boldsymbol{d}}\times\boldsymbol{c})^T] \\ &\quad = [\dot{\boldsymbol{c}}^T \quad \mathbf{0}_{1\times3}] + [\mathbf{0}_{1\times3} \quad (\boldsymbol{d}\times\dot{\boldsymbol{c}})^T + (\dot{\boldsymbol{d}}\times\boldsymbol{c})^T] \\ &\quad = \boldsymbol{V}^T\mathbf{h}_6, \\ &\mathbf{h}_6 = \begin{bmatrix}\mathbf{0}_{3\times3} & \mathbf{0}_{3\times3} \\ \mathbf{J}_c^T & (\hat{\mathbf{d}}\mathbf{J}_c)^T\end{bmatrix}_{6\times6} - \begin{bmatrix}\mathbf{0}_{6\times3} & (\hat{\mathbf{c}}\mathbf{J}_d)^T\end{bmatrix}_{6\times6}.\end{aligned} \tag{16g}$$

Combining Eq. (14b) with Eqs. (15b), (15c), and (16g), an inverse acceleration $\boldsymbol{a}_{in}$ and a forward acceleration $\boldsymbol{A}$ and a Hessian matrix $\mathbf{H}$ are derived as follows:

$$\begin{aligned}\boldsymbol{a}_{in} &= \mathbf{J}\boldsymbol{A} + \boldsymbol{V}^T\mathbf{H}\boldsymbol{V}, \\ \boldsymbol{A} &= \mathbf{J}^{-1}(\boldsymbol{a}_{in} - \boldsymbol{V}^T\mathbf{H}\boldsymbol{V}), \\ \boldsymbol{a}_{in} &= [a_{r1} \quad a_{r2} \quad a_{r3} \quad \ddot{\alpha} \quad \ddot{\lambda} \quad 0]^T, \\ \mathbf{H} &= [\mathbf{h}_1 \quad \mathbf{h}_2 \quad \mathbf{h}_3 \quad \mathbf{h}_4 \quad \mathbf{h}_5 \quad \mathbf{h}_6]^T.\end{aligned} \tag{17}$$

6. Reachable Workspace and Orientation

A reachable workspace W of the 2SPS+UPU PM is defined as all positions that can be reached by the central point of m. When given the maximum extension $r_{\max}$ and the minimum extension $r_{\min}$ of active legs r_i $(i = 1, 2, 3)$, W can be constructed using its simulation mechanism or some relative analytic formulae. In fact, W is formed by a family of similar spatial surfaces, which are cascaded from a lower boundary surface S_l to an upper boundary surface S_u by using the loft command.

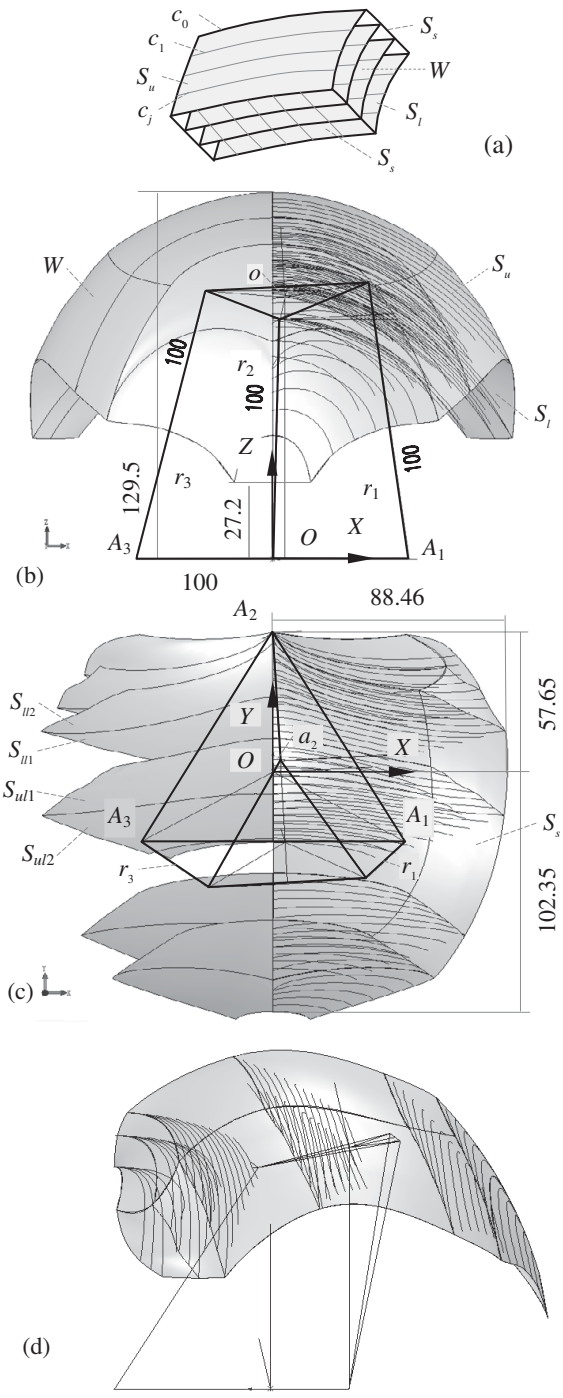

Fig. 4. The plane symmetry reachable workspace of the 2SPS+UPU PM. (a) A family of similar surfaces cascaded from a lower boundary surface S_l to an upper boundary surface S_u. (b) The front view. (c) The top of view. (d) The side view.

Each of the similar spatial surfaces is formed by a family of similar spatial curves c_j $(j = 0, 1, \ldots, n_1 - 1)$ using the loft command,[11] see Fig. 4(a).

Since the 2SPS+UPU PM has a symmetric plane of O-YZ in structure, its W must be of plane symmetry of O-YZ. Therefore, only an upper-left boundary surface S_{ul}

and a lower-left boundary surface S_{ll} are constructed. The construction procedures are explained as follows:

Step 1. Set $L = 100$, $l = 60$, $r_{\max} = 130$, $r_{\min} = 100$, $\delta r = 5$ cm, and $n_1 = (r_{\max} - r_{\min})/\delta r$, $\theta = 90^\circ$ (the angle θ between lines r_2 and y).
Step 2. Set $r_1 = r_{\min}$, $r_2 = r_{\max}$, $r_3 = r_{\min} + j\delta r$ ($j = 0, 1, \ldots, n_1 - 1$).
Step 3. Set $j = 0$, increase α from 0 by $\delta\alpha$ at each increment step, and inspect the interferences among r_i and m in the simulation mechanism. When the interferences occur, stop increasing α.
Step 4. Solve the position components (X_o, Y_o, Z_o) of m in $\{B\}$ using automatically solving function of Solidworks or relevant equations, and insert them into the simulation mechanism.
Step 5. Construct a spatial curve c_0 using the curve pass through *XYZ* command.
Step 6. Repeat the steps 3 through 5 above, except that set $j = 1, \ldots, n_1$, respectively. Thus, other curves c_j are created.
Step 7. Construct the first upper-left boundary surface S_{ul1} from n_1 curves c_j ($j = 0, 1, \ldots n_1 - 1$) by the surface loft command.
Step 8. Using similar construction procedures of S_{ul1}, construct the second upper-left boundary surface S_{ul2}, except that setting $r_1 = r_{\max}$.
Step 9. Using similar construction procedures of S_{ul1} and S_{ul2}, construct the two lower-right boundary surfaces S_{ll1} and S_{ll2}, except that setting $r_2 = r_{\min}$.
Step 10. Construct S_{ul} from S_{ul1} and S_{ul2}. Construct S_{ll} from S_{ll1} and S_{ll2}.
Step 11. Using the mirror command vs. plane *O-YZ*, construct an upper boundary surface ${}^1S_u$ from S_{ul} and a lower boundary surface ${}^1S_l$ from S_{ll}, see Figs. 4(b) and (c).
Step 12. Repeat the steps 2 through 11, construct other surfaces ${}^jS_u$ and ${}^jS_l$ ($j = 2, 3, 4, 5$), except set $\theta = 160^\circ$, 135° , 75° , 60° , respectively.
Step 13. Construct W from ${}^jS_u$ and ${}^jS_l$ ($j = 2, 3, 4, 5$) using the loft command.

The results show that W is symmetric about the *O-YZ* plane and it is larger than that of the 4SPS+SPR PM.[11]

6.1. Examples

Set $L = 100$, $l = 60$ cm, $\boldsymbol{F} = -[20, 30, 60]^T$ kN, $\boldsymbol{T} = [-30\ -30, 100]^T$ kN·cm. When given five pose parameters (α, β, λ, Y_o Z_o), see Figs. 5(a) and (b), the extension, the velocity, and the acceleration of active legs r_i are solved using Matlab, see Figs. 5(b)–(d). The forward velocity and acceleration of m are solved, see Figs. 5(e) and (f). The three active forces F_{ai} ($i = 1, 2, 3$) and one constraint force F_c are solved, see Fig. 5(g). Two active torques T_a T_λ, one constraint torque T_c, and one bending moment T_b are solved, see Fig. 5(h). The results have been verified by its force simulation mechanism.

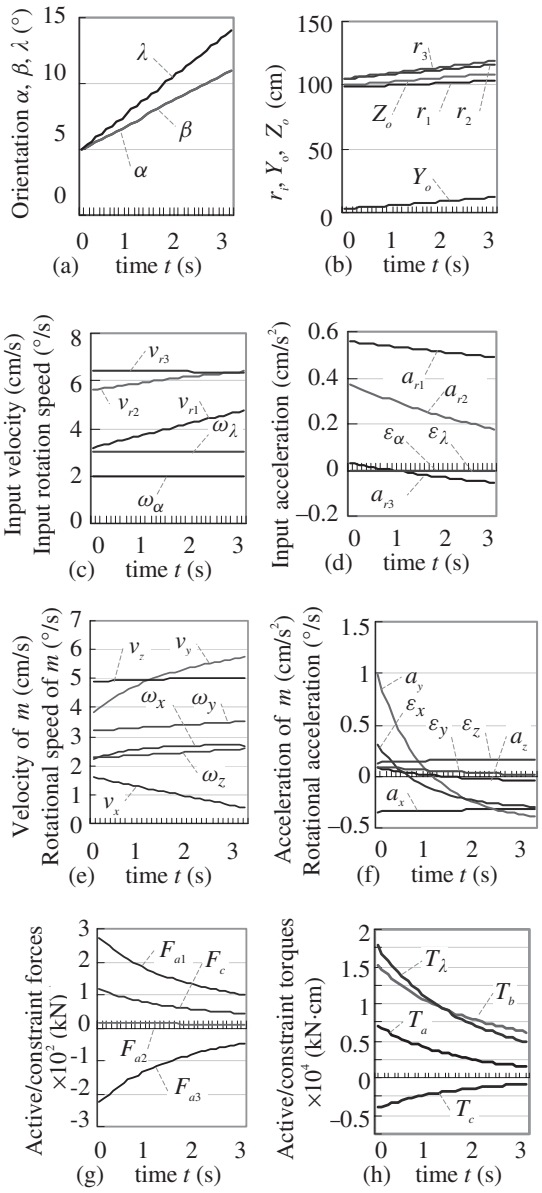

Fig. 5. Solved results of 2SPS+UPU PM.

7. Conclusions

A 2SPS+UPU PM with two SPS-type active legs and one UPU-type composite active constrained leg has five DoFs, i.e., four rotations and one translation. The whole structure is simplified, the interference among the active legs and platform can be avoided easily, and the workspace may be increased.

Each of the SPS-type active legs with the linear actuator is simple in structure and has a relative large capability of load bearing. The UPU-type composite active constrained leg is composed of a linear actuator and two rotational actuators, it can effectively remove tiny self-motion.

The reachable workspace of the 2SPS+UPU PM is symmetric about the *O-YZ* plane and is larger than that of the 4SPS+SPR PM.

A 6 × 6 Jacobian matrix without the first-order partial differentiation and a six layer 6 × 6 Hessian matrix without the second-order partial differentiation are derived, and the inverse/forward velocity and acceleration of the 2SPS+UPU PM are solved. The analytic results of the 2SPS+UPU PM are verified by its simulation mechanism.

The 2SPS+UPU PM has some potential applications for the 5-DoF parallel machine tools, the 5-DoF sensor, the

surgical manipulator, the tunnel borer, the barbette of war ship, and the satellite surveillance platform.

Acknowledgments

The authors would like to acknowledge a project (51175447) supported by National Natural Science Foundation of China and a key planned project of Hebei application foundation (11962127D) and a project (2011-O02) supported by State Key Laboratory of Robotics.

References

1. J. P. Merlet, *Parallel Robots*, 2nd ed. (Springer, Netherlands, 2006).
2. Z. Huang, L. F. Kong and Y. F. Fang, *Theory on Parallel Robotics and Control* (Machinery Industry Press, Beijing, China, 1997).
3. Y. Fang and L. W. Tsai, "Structure synthesis of a class of 4-dof and 5-dof parallel manipulators with identical limb structures," *Int. J. Robot. Res.* **21**(9), 799–810 (2002).
4. X. Kong and C. M. Gosselin, "Type synthesis of 5-DOF parallel manipulators based on screw theory," *J. Robot. Syst.* **22**(10), 535–547 (2005).
5. T. Huang, M. Li, X. M. Zhao, J. P. Mei, D. G. Chetwynd and S. J. Hu, "Conceptual design and dimensional synthesis for a 3-DOF module of the TriVariant—A novel 5-DOF reconfigurable hybrid robot," *IEEE Trans. Robot.* **21**(3), 449–456 (2005).
6. Q. C. Li, Z. Huang and J. M. Hervé, "Type synthesis of 3R2T 5-dof parallel mechanisms using Lie group of displacements," *IEEE Trans. Robot. Autom.* **20**(2), 173–180 (2004).
7. F. Gao, W. Li and X. C. Zhao, "New kinematic structures for 2-, 3-, 4-, and 5-DOF parallel manipulator designs," *Mech. Mach. Theory* **37**(11), 1395–1411 (2002).
8. D. Zhang and C. M. Gosselin, "Kinetostatic modeling of N-DOF parallel mechanisms with a passive constraining leg and prismatic actuators," *ASME J. Mech. Des.* **123**(3), 375–384 (2001).
9. R. I. Alizade and C. Bayram, "Structural synthesis of parallel manipulators," *Mech. Mach. Theory* **39**(8), 857–870 (2004).
10. Y. Lu and B. Hu, "Unification and simplification of velocity/acceleration of limited-dof parallel manipulators with linear active legs," *Mech. Mach. Theory* **43**(9), 1112–1128 (2008).
11. Y. Lu, H. Bo and J. Y. Xu, "Kinematics analysis and solution of active/passive forces of a 4SPS + SPR parallel machine tool," *Int. J. Adv. Manuf. Technol.* **42**(7–8), 804–812 (2009).
12. H. Chanhee, K. Jinwook, K. Jongwon and F. C. Park, "Kinematic sensitivity analysis of the 3-UPU parallel mechanism," *Mech. Mach. Theory* **37**(8), 787–798 (2002).
13. P. Ji and H. T. Wu, "Kinematics analysis of an offset 3-UPU translational parallel robotic manipulator," *Robot. Autom. Syst.* **42**(2), 117–123 (2003).
14. D. Now, "A Newton-Euler formulation for the inverse dynamics of the Stewart platform manipulator," *Mech. Mach. Theory* **33**(8), 1135–1152 (1998).
15. L. W. Tsai, "Solving the inverse dynamics of a Stewart-Gough manipulator by the principle of virtual work," *Trans. ASME J. Mech. Des.* **122**(1), 3–9 (2000).
16. J. Gallardo, J. M. Rico, A. Frisoli, D. Checcacci and M. Bergamasco, "Dynamics of parallel manipulators by means of screw theory," *Mech. Mach. Theory* **38**(11), 1113–1131 (2003).
17. J. S. Dai, Z. Huang and L. Harvey, "Mobility of over constrained parallel mechanisms," *ASME J. Mech. Des.* **128**(1), 220–229 (2006).
18. Y. Lu and B. Hu, "Analysis of kinematics and solution of active/constrained forces of asymmetric 2UPU + X parallel manipulators," *J. Mech. Eng. Sci.* (Proc. IMechE Part C) **220**(C12), 1819–1830 (2006).
19. R. Di Gregorio, "Kinematics of the 3-UPU wrist," *Mech. Mach. Theory* **38**(3), 253–263 (2003).
20. Z. Huang, S. H. Li and R. G. Zou, "Feasible instantaneous motions and kinematic characteristics of a special 3-DOF 3-UPU parallel manipulator," *Mech. Mach. Theory* **39**(9), 957–970 (2004).
21. R. Andrea, S. Rosario and X. Fengfeng, "Static balancing of parallel robots," *Mech. Mach. Theory* **40**(2), 191–202 (2005).
22. S. Ider, "Kemal Inverse dynamics of parallel manipulators in the presence of drive singularities," *Mech. Mach. Theory* **40**(5), 578–599 (2005).
23. D. Chakarov, "Study of the passive compliance of parallel manipulators," *Mech. Mach. Theory* **34**(3), 373–389 (1999).
24. M. Li, T. Huang, J. Mei, X. Zhao, D. G. Chetwynd and H S. Jack, "Dynamic formulation and performance comparison of the 3-DOF modules of two reconfigurable PKM—The Tricept and the TriVariant," *ASME J. Mech. Des.* **127**(5), 1129–1136 (2005).
25. G. Alici and B. Shirinzadeh, "Topology optimisation and singularity analysis of a 3-SPS parallel manipulator with a passive constraining spherical joint," *Mech. Mach. Theory* **39**(2), 215–235 (2004).

Appendix: The creation processes of simulation mechanism

1. Construct B in 2D sketch. The subprocedures are: a. Construct an equilateral triangle $\Delta A_1A_2A_3$ by the polygon command. b. Coincide its central point O with origin of default coordinate, set its one side horizontally, and give its one side a fixed dimension $L_i = 100$ cm in length. c. Transform $\Delta A_1A_2A_3$ into a plane.
2. Construct m in 3D sketch. The subprocedures are: a. Create three lines l_i ($i = 1, 2, 3$), and connect them to form a closed triangle $\Delta a_1a_2a_3$. b. Give each of l_i the same initial dimension $l = 60$ cm. c. Create a line y, connect its two ends to a_2 and l_2. d. Create a line e, connect its two ends to a_3 and y at point o. e. Set $y \perp e$ and $e \perp l_2$.
3. Construct two SPS-type active legs. The subprocedures are: a. Construct two lines r_i ($i = 1, 3$), and connect their two ends to m at a_i and to B at A_i. b. Give each of r_i the initial driving dimension.
4. Take the default coordinate O-XYZ as a fixed coordinate on B, based three Euler rotations of (ZX_1Y_2), construct three coordinate systems O-$X_iY_iZ_i$ ($i = 1, 2, 3$). Set $X_1 \perp Z$, $Y_2 \| y$, and $Z_3 \| z$.
5. Construct a UPU-type active leg. The subprocedures are: a. Construct a line r_2, and connect its two ends to m at a_2 and to B at A_2. b. Construct a line R_2, and connect its one end to B at A_2. d. Construct a line R_3, connect its one end to m at a_2. e. Set $R_2 \| X_1$, $R_3 \| X_1$, $R_2 \perp r_2$, $R_3 \perp r_2$, and $R_3 \perp y$.
6. Construct a line Z_o, connect its two ends to m at o and to B at point A_o, and set $Z_o \perp B$. Give each of distances from A_o to Y, X, and o the driven dimensions. Construct a line c, connect its one end to m at a_3 and set $c \| R_3$. Give the angle α between X and X_1, and the angle λ between c and l_2 driving dimensions. Give the angle β between Y_1 and Y_2, the driven dimension.

When varying the driving dimensions of r_i ($i = 1, 2, 3$) and the angle α and the angle λ, (X_o Y_o Z_o) of m in $\{B\}$ of the 2SPS+UPU PM are solved automatically. At the same time, the orientation components β of m in $\{B\}$ are solved automatically.